

Coherent control of microwave pulse storage in superconducting circuits

Patrick M. Leung and Barry C. Sanders

*Institute for Quantum Information Science,
University of Calgary, Alberta T2N 1N4, Canada*

Abstract

Coherent pulse control for quantum memory is viable in the optical domain but nascent in microwave quantum circuits. We show how to realize coherent storage and on-demand pulse retrieval entirely within a superconducting circuit by exploiting and extending existing electromagnetically induced transparency technology in superconducting quantum circuits. Our scheme employs a linear array of superconducting artificial atoms coupled to a microwave transmission line.

PACS numbers: 42.50.Gy, 03.67.Mn, 85.25.Hv

Circuit quantum electrodynamics has successfully realized numerous quantum optical phenomena in the microwave (μw) domain [1] and is a promising architecture for quantum information technology [2]. Various superconducting artificial atoms (SAAs) have been realized including Cooper pair boxes [3], transmons [4], flux qubits [5] and fluxonium [6]. These SAAs can be coupled to a μw transmission line that serves as a ‘quantum bus’ for μw photons [7]. For efficient large-scale quantum information processing, synchronization of information flow between highly separated SAAs requires the μw photons to be stored in quantum memories [8] coherently and retrieved on-demand.

One strategy is to couple the superconducting circuit to external spin- $\frac{1}{2}$ systems [9] so that quantum information stored in the μw field can be transferred for on-demand storage and retrieval [10]. Exciting progress has been made in this direction by coupling the superconducting circuit to nitrogen vacancies in diamond [11]. However, due to inhomogeneous broadening, the storage time is still limited to ~ 30 ns [12], which is insufficient for quantum memory. Moreover, hybridizing with another quantum information medium adds extra complexity to the fabrication process. We propose an alternative strategy that avoids hybridization and instead builds quantum-field storage and memory into the superconducting circuit itself. Specifically we propose the creation of a linear array of SAAs coupled to the transmission line, with this array serving as a pulse storage and on-demand retrieval medium. Our scheme is similar to quantum memory approaches in atomic systems [13] and leverages off recent experimental demonstrations of superconducting-circuit electromagnetically induced transparency (EIT) [14]. The point of our scheme is to create μw quantum memory in a superconducting circuit without the need to hybridize media, akin to the optical case with atomic quantum memory [8].

Although various choices of SAAs are available, we explore using fluxonium artificial atoms [6] because they can serve as highly-coherent three-level SAAs [15]. Three-level atoms are particularly amenable to μw -field control via Autler-Townes splitting or EIT [16]. As illustrated in Fig. 1(a), in our model, n SAAs are periodically spaced with inter-atomic distance l optimized to yield maximum storage efficiency. The total medium length is $d = (n - 1)l$. Aperiodic spacings affect the position of the scattering resonances in the EIT spectra but do not alter the efficacy of our scheme. We shall see that interference due to inter-SAA scattering modifies the transmission spectrum in a geometry-dependent way, but these complex spectral features are not an obstacle to realizing μw pulse storage and

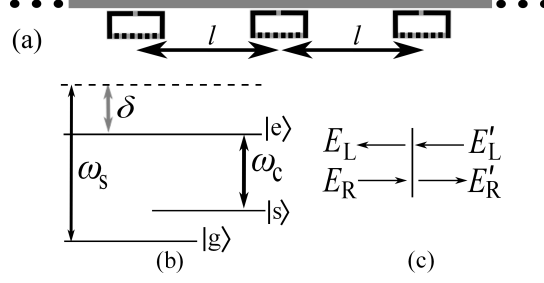


FIG. 1: (a) Linear array of fluxonium (rectangles with dashed side) periodically spaced with separation l and coupled to (gray) transmission line. (b) Three energy levels of the fluxonium SAA with on-resonant control driving of the $|e\rangle \leftrightarrow |s\rangle$ transition with frequency ω_c and off-resonant driving of the $|e\rangle \leftrightarrow |g\rangle$ transition with frequency ω_s and detuning δ . (c) Incoming and outgoing fields (indicated by arrow direction) for one SAA labeled by field amplitudes E_R and E'_L for incoming fields and E_L and E'_R for outgoing, with L and R denoting ‘left’ and ‘right’, respectively.

retrieval.

The energy levels $|g\rangle$, $|s\rangle$ and $|e\rangle$ and driving fields for a three-level SAA are depicted in Fig. 1(b) for each fluxonium SAA. Two driving fields are required to realize EIT. The control field frequency ω_c is resonant with ω_{es} (with ω_{xy} the frequency for transition $|x\rangle \leftrightarrow |y\rangle$ and $x,y \in \{g,s,e\}$) and a signal field of frequency ω_s detuned by $\delta = \omega_s - \omega_{eg}$ from ω_{eg} . When the control field is off, the SAA is opaque to the signal field; turning on the control field makes the SAA transparent. In addition, this three-level SAA can yield ‘EIT with amplification’ [17].

Previous studies focusing on EIT in superconducting circuits concentrate on the case of a single SAA and predict [18] and demonstrate [14] changes to the transmission and reflection characteristics of the single atom but do not consider phenomena such as slow light and properties such as optical depth that are crucial for building quantum memory. Here we consider a linear array of n SAAs to enable on-demand storage and retrieval of μW pulses. A large-amplitude, long-duration μW control field pumps the medium in order to prepare coherence between SAA energy levels in advance of the arrival of the μW signal pulse. This coherence suppresses the absorption of the small-amplitude signal pulse as well as slowing the signal propagation, thereby allowing the pulse to enter the transparent medium slowly.

Once the signal pulse is contained within the medium, the pulse is trapped by turning off the control field. Subsequently, turning on the control field enables retrieval of the signal

pulse on-demand. This method of μw pulse storage in a quantum circuit is inspired by the technique for storing an optical pulse in an EIT-enabled medium [19], which means the artificial atomic medium requires large optical depth for high storage efficiency [8], and we show that our array of SAAs is capable of delivering the requisite optical depth.

As the medium is one-dimensional (1D), the incoming signal fields encountering a SAA are scattered into transmitted and reflected components as depicted in Fig. 1(c). For a strong non-depleting control field with constant Rabi frequency modulus $|\Omega|$ throughout the medium, the reflection coefficient $r(\delta)$ for the signal field scattering from a SAA is [20]

$$r = \frac{\Gamma_{\text{eg}}}{2(\Gamma_{\text{e}} - i\delta) + \frac{|\Omega|^2}{2(\Gamma_{\text{s}} - i\delta)}}, \Gamma_{\text{e}} = \frac{\Gamma_{\text{eg}} + \Gamma_{\text{es}}}{2}, \Gamma_{\text{s}} = \frac{\Gamma_{\text{sg}}}{2}, \quad (1)$$

with Γ_{xy} the decay rate for the $|x\rangle \leftrightarrow |y\rangle$ transition. The transmission coefficient is $t = 1 - r$. By treating the SAAs as point scatterers with linear susceptibilities, each SAA acts as a boundary for the transmission and reflection components of the signal field. Therefore, we apply the reflection-and-transmission transfer matrix method [21] to calculate the transmission through a sequence of SAAs. For a single SAA, the induced transformation of the signal field is

$$t(\delta) \begin{pmatrix} E_{\text{R}}(\delta) \\ E_{\text{L}}(\delta) \end{pmatrix} = \begin{pmatrix} 1 & -r(\delta) \\ r(\delta) & t^2(\delta) - r^2(\delta) \end{pmatrix} \begin{pmatrix} E'_{\text{R}}(\delta) \\ E'_{\text{L}}(\delta) \end{pmatrix}. \quad (2)$$

We include phase shift $\varphi = l\omega_{\text{s}}/c$, taking into account the free propagation of the signal field between SAAs through the transmission line at speed c . The overall transformation by the linear array, denoted as matrix M , is given by

$$\begin{pmatrix} E_{1\text{R}}(\delta) \\ E_{1\text{L}}(\delta) \end{pmatrix} = M(\delta) \begin{pmatrix} E'_{n\text{R}}(\delta) \\ E'_{n\text{L}}(\delta) \end{pmatrix} \quad (3)$$

for the subscript 1 denoting the first SAA and n the last SAA of the n -SAA array.

As $E_{\text{in}} := E_{1\text{R}}$ is the only nonzero input field, $E'_{n\text{L}} = 0$, only the upper-left element of the response matrix

$$\begin{aligned} M_{11} &= \frac{(A_+ + B)(A_- + B)^n - (A_+ - B)(A_- - B)^n}{2^{n+1}e^{i(n-1)\varphi}B(r-1)^n}, \\ A_{\pm} &= \pm e^{2i\varphi}(1 - 2r) - 1, \\ B &= \sqrt{(e^{2i\varphi} - 1)(e^{2i\varphi}(1 - 2r)^2 - 1)} \end{aligned} \quad (4)$$

is needed to obtain the output signal field $E_{\text{out}} = E_{\text{in}}/M_{11}$, with transmission $T = |1/M_{11}|^2$.

Let us now consider an example of how this system works by judiciously choosing favorable yet realistic parameters. The transition frequency values are $\omega_{\text{eg}}/2\pi = 10.4$ GHz and $\omega_{\text{es}}/2\pi = 6.99$ GHz at flux bias $\Phi = 0.32\Phi_0$ for $\Phi_0 \equiv h/2e$ the flux quantum; this flux bias yields long coherence times [15]. The $|e\rangle \leftrightarrow |g\rangle$ transition wavelength is $\lambda = 2\pi c/\omega_{\text{eg}} = 5.79$ mm and $c = 6 \times 10^7$ m/s. We treat decoherence as being due fundamentally to spontaneous emission [20]. Using Manucharyan et al.'s [15] measured relaxation parameter $\Gamma_{\text{sg}} \approx 0.167$ MHz, we calculate the fluxonium relaxation parameters to be $\Gamma_{\text{eg}} = 173\Gamma_{\text{sg}}$ and $\Gamma_{\text{es}} = 40\Gamma_{\text{sg}}$ [24].

The field transmission in a translucent medium is related to the optical depth α by $T = e^{-\alpha}$. For equally spaced atoms, the length of the medium increases as n increases and Beer's Law holds if $\alpha \propto n$. For the choice of parameters and for two choices of inter-SAA separation l , at $\lambda/4$ and at one other value, we can see in Fig. 2(a) that the optical depth at $\delta = 0$ with control field off ($\Omega = 0$) is a linear function of n in accordance with Beer's Law; additional modulation due to inter-SAA scattering interference is negligible. For even a dozen SAAs the optical depth is high compared to typical optical depths in optical-EIT of less than 25 [22]. From equation (4), we find that the medium absorbs the signal field maximally when $l \rightarrow (2m+1)\lambda/4$, where m is any non-negative integer. An exception to Beer's Law occurs when $l \rightarrow m\lambda/2$, in which $\alpha \rightarrow 2\ln\left(\frac{1+(n-1)r(0)}{1-r(0)}\right)$.

Inter-SAA scattering interference occurs during transmission of a μW field through a periodic array of fluxonium SAAs, which may have complications that are absent in optical-EIT. We explore the effect that inter-SAA scattering interference has on EIT within the 1D array of fluxonium SAAs as depicted in Figs. 3(a) and 3(b). Due to interference effects, in Fig. 3(a) the transmission profiles with and without the control field on are markedly different from Fig. 3(b). Fig. 3(b) is plotted using identical conditions as for Fig. 3(a) except with a different inter-SAA spacing. In Fig. 3(a) scattering creates asymmetry and oscillations but the EIT features remain intact. Fig. 3(b) looks like textbook EIT, with $1-T$ replacing absorption, which is realized by choosing some appropriate inter-SAA spacings.

In our scheme, the μW input signal field is a pulse, and its speed is quantified by the group velocity. The transmitted signal pulse acquires a phase factor e^{ikd} from propagation through the medium, and the dispersion relation and group velocity are

$$k(\omega_s) = \frac{1}{d} \arg\left(\frac{1}{M_{11}(\omega_s)}\right), \quad v_g = \left(\frac{dk}{d\omega_s}\right)_{\delta=0}^{-1}, \quad (5)$$

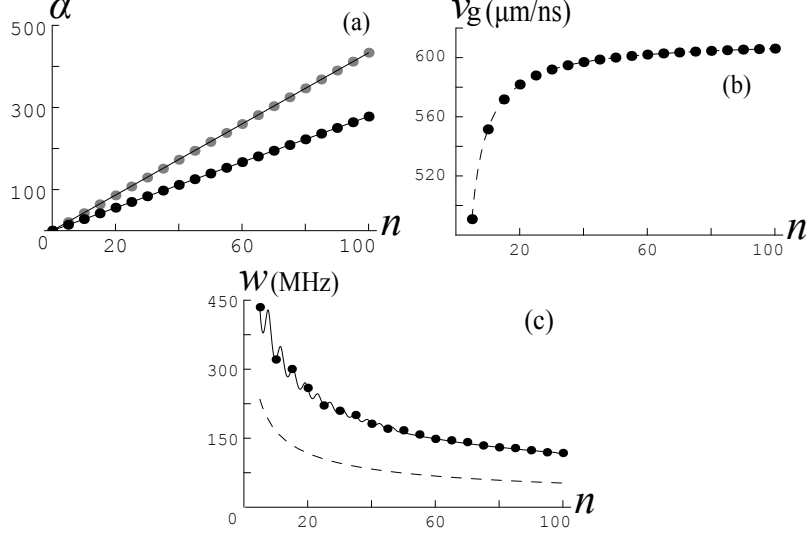


FIG. 2: Characteristics of a periodically spaced SAA array with n atoms and inter-SAA separation l . (a) Optical depth α vs n for $l = \lambda/4 = 1.45$ mm (gray dots) fitted to a straight line $\alpha = 4.33n$ and for $l = 0.370$ mm (black dots) fitted to straight line $\alpha = 2.78n$. For (b-c) the relevant parameters are $l = 0.748$ mm and the control-field Rabi frequency is $\Omega = 218$ MHz with numerical evaluation (dots) and the optical-EIT formulae (dashed). (b) Group velocity of a pulse through the array. (c) EIT window width w vs n . Analytical evaluation (solid) of w using Eq. (6) shows oscillatory behavior.

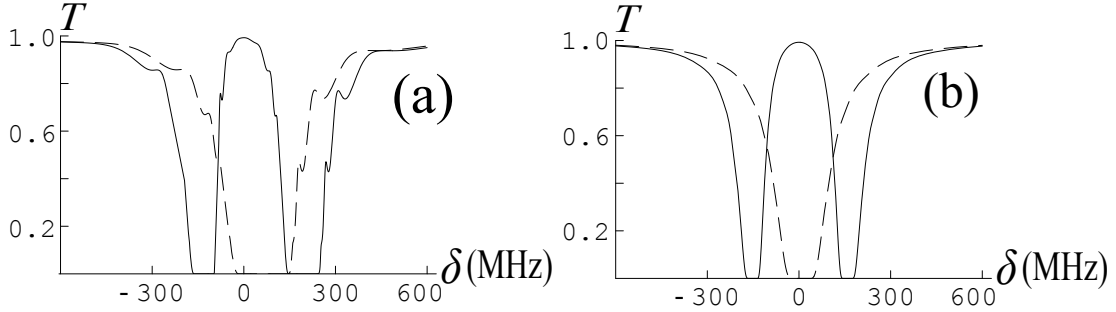


FIG. 3: Transmission through $n = 100$ fluxonium SAAs with inter-SAA separation (a) $l = 0.15$ mm and (b) $l = 0.7$ mm for $\Omega = 0$ (dashed) and with $\Omega = 309$ MHz (solid).

respectively. Based on $T = T_{\delta=0} \exp(-\delta^2/w^2)$ [23] with $T_{\delta=0} \approx 1$, which holds for small δ (i.e. in the vicinity of the EIT window), the EIT window width w is given by

$$w^2 = -2 \left(\frac{d^2 \ln T}{d\delta^2} \bigg|_{\delta=0} \right)^{-1}. \quad (6)$$

Using Eqs. (5) and (6), we determine the inter-SAA scattering-included group velocity and

EIT window width. Furthermore, we determine the group velocity and the width for the case of negligible inter-SAA scattering as in optical EIT. When EIT occurs, within the EIT window, the reflection of signal due to each SAA is small. Therefore, for the case of negligible inter-SAA scattering, the overall transmission coefficient is $M_{11}^{-1} = (1 - r)^n e^{i(n-1)\varphi}$ and the resultant transmission is $T \approx e^{-2n\text{Re}(r)}$. Hence we have

$$w \approx \frac{|\Omega|^2}{4\Gamma_{\text{eg}}\beta\sqrt{2n}}, \beta = |\Omega|^2 \sqrt{\frac{(\Gamma_e + 2\Gamma_s)|\Omega|^2 - 4\Gamma_s^3}{2\Gamma_{\text{eg}}(4\Gamma_e\Gamma_s + |\Omega|^2)^3}}. \quad (7)$$

For χ the linear susceptibility, the overall transmission coefficient is $M_{11}^{-1} = e^{i\omega_s \chi d/(2c)} e^{i(n-1)\varphi}$ [23] so

$$v_g = \left(\frac{1}{c} + \frac{2n\Gamma_{\text{eg}}}{(n-1)l|\Omega|^2} \right)^{-1}. \quad (8)$$

Equations (7) and (8) are the 1D version of the EIT window width and group velocity expressions from optical-EIT theory [23], and we refer to these two equations as optical-EIT formulae. We evaluate the scattering-included v_g and w and compare them against optical-EIT formulae in Figs. 2(b-c), respectively, to see how closely the optical-EIT formulae apply in the case of a μW pulse propagating through a fluxonium array. The agreement between the inter-SAA scattering-free theory and scattering-included theory shows that, with the chosen parameters, inter-SAA scattering interference has negligible effect on the group velocity. Furthermore, for the case of including scattering, w is larger with $w \propto \frac{1}{\sqrt{n}}$ plus an additional modulation due to inter-SAA scattering, which appears as oscillations that dampens exponentially as n increases (details in Appendix).

To show that storage of a μW pulse in the fluxonium SAA array is indeed possible using the EIT phenomenon, we consider an input pulse whose spectral profile is Gaussian with respect to detuning δ with $\delta = 0$ corresponding to input frequency ω_{eg} . The spectral function for the dimensionless input field is thus a Gaussian function $E_{\text{in}}(\delta)$ with standard deviation σ and normalized field strength according to $\int |E_{\text{in}}(\delta)|^2 d\delta = 1$. In our numerical evaluation, we determine the pulse storage efficiency $\eta(n, \Omega, l, \sigma)$, which is defined as the percentage of the pulse trapped inside the medium as soon as the control field is turned off.

We now employ the following conditions to evaluate the efficiency under reasonable experimental conditions. As the medium must be sufficiently transparent when the pulse enters, we set Ω such that $T_{\varphi \rightarrow 0} = 0.99$ at $\delta = 0$. We require that $v_g \ll c$ when the control field is on, which is guaranteed by choosing l such that $v_g \approx c/100$ from Eq. (8). Not only does this

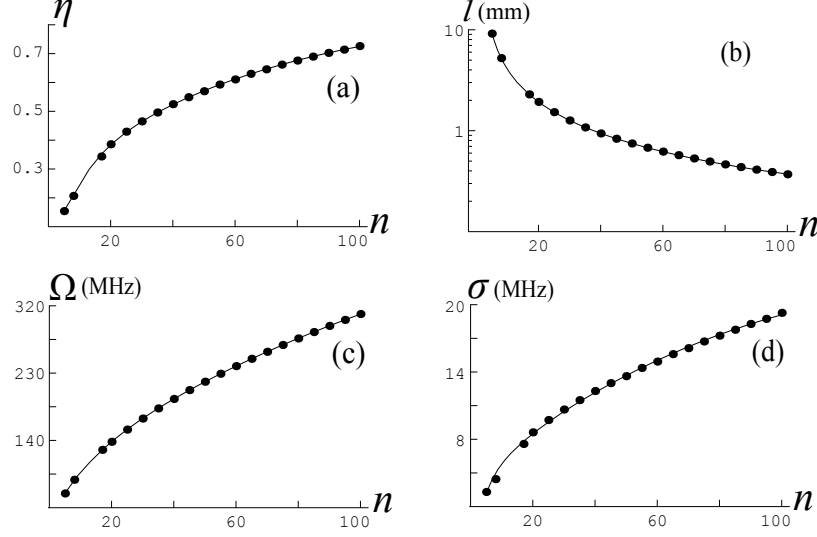


FIG. 4: (a) Optimal storage efficiency for n SAAs. Solid line is an interpolated fit. (b) Corresponding atomic separation l . (c) Corresponding control field Rabi frequency. (d) Corresponding standard deviation of the Gaussian spectral profile of the input pulse.

condition ensure that the pulse is slowed inside the medium but also assures that the control field can be switched off to make the medium opaque before the pulse escapes. The pulse must fit inside the EIT spectral window so we choose σ such that $\int |E_{\text{out}}(\delta)|^2 d\delta \approx 0.98$ as a benchmark. If the pulse is temporally longer than the available time window d/v_g , only the central part of the pulse within this time window is stored and the pulse storage efficiency is reduced.

Storage efficiency vs n is shown in Fig. 4(a). The corresponding values of atomic separation l , control field Rabi frequency Ω and the standard deviation of the pulse σ from the constraining conditions are shown in Figs. 4(b-d) respectively. Although some of the separation values in Fig. 4(b) do lead to distortion in the EIT spectra as in Fig. 3(a), the effect on the efficiency is negligible with the corresponding pulse widths. As the number of SAAs increases, the pulse storage efficiency increases as expected. For five SAAs, the efficiency is $\eta \approx 0.15$, and for $n = 100$, the efficiency is $\eta \approx 0.72$, which is comparable to the (retrieval) efficiency observed in optical-EIT pulse storage medium [22]. Asymptotically, η approaches near unity as n becomes large. For example we evaluate the efficiency for $n = 300$ and find that $\eta \approx 0.91$. Therefore, pulse storage is possible with a few SAAs and asymptotically efficient with increasing number of SAAs.

In conclusion, we have shown that coherent storage and on-demand pulse retrieval are feasible using existing superconducting artificial atom technology [6] provided that an array of sufficiently large number of the artificial atoms is constructed as suggested. Our scheme obviates the need to hybridize the technology, e.g. by coupling to nitrogen-vacancy diamond defects [11]. Hybridizing is a promising approach but introduces unwanted complexity and the storage time is limited by inhomogeneous broadening. Our scheme is surprisingly efficient even for few artificial atoms, for example delivering 15% efficiency with just five artificial atoms. This efficiency is dramatically improved with more atoms and ultimately reaches near unit efficiency asymptotically. Our scattering-free 1D optical-EIT equations provide a good guideline for how to construct quantum memory in superconducting circuits. Numerical evaluations are then necessary to assure that the theory gives quantitative agreement with experiments. Our results are important for information synchronization and quantum memory in superconducting circuits, which are one of the most promising quantum computing technologies.

ACKNOWLEDGEMENT

We appreciate financial support from AITF, NSERC and CIFAR, and valuable discussions with A. Blais and J. Joo.

-
- [1] M. Baur et al., Phys. Rev. Lett. **102**, 243602 (2009); M. A. Sillanpää et al., *ibid* **103**, 193601 (2009); W. R. Kelly et al., *ibid* **104**, 163601 (2010).
 - [2] A. Zagoskin and A. Blais, Phys. Canada **63**, 215 (2007).
 - [3] Y. Nakamura, Yu. A. Pashkin and J. S. Tsai, Nature **398**, 786 (1999).
 - [4] J. Koch et al., Phys. Rev. A **76**, 042319 (2007).
 - [5] I. Chiorescu, Y. Nakamura, C. J. P. M. Harmans and J. E. Mooij, Science **299**, 1869 (2003).
 - [6] V. E. Manucharyan, J. Koch, L. I. Glazman and M. H. Devoret, Science **326** **113** (2009).
 - [7] J. Majer et al., Nature **449**, 443 (2007).
 - [8] A. I. Lvovsky, B. C. Sanders and W. Tittel, Nature Phot. **3**, 706 (2009).
 - [9] P. Rabl et al., Phys. Rev. Lett. **97**, 033003 (2006); D.I. Schuster et al., Phys. Rev. Lett. **105**,

- 140501 (2010).
- [10] H. Wu et al., Phys. Rev. Lett. **105**, 140503 (2010).
 - [11] Y. Kubo et al., Phys. Rev. Lett. **105**, 140502 (2010); X. Zhu et al., Nature **478**, 221 (2011);
Y. Kubo et al., Phys. Rev. Lett. **107**, 220501 (2011).
 - [12] Y. Kubo et al., Phys. Rev. A **85**, 012333 (2012).
 - [13] M. Bajcsy, A. S. Zibrov and M. D. Lukin, Nature **426**, 638 (2003).
 - [14] A. A. Abdumalikov Jr. et al., Phys. Rev. Lett. **104**, 193601 (2010).
 - [15] V. E. Manucharyan et al., arXiv:1012.1928 (2010).
 - [16] P. M. Anisimov, J. P. Dowling and B. C. Sanders, Phys. Rev. Lett. **107**, 163604 (2011).
 - [17] J. Joo, J. Bourassa, A. Blais and B. C. Sanders, Phys. Rev. Lett. **105**, 073601 (2010).
 - [18] K. V. R. M. Murali et al., Phys. Rev. Lett. **93**, 087003 (2004).
 - [19] M. Fleischhauer, A. Imamoglu and J. P. Marangos, Rev. Mod. Phys. **77**, 633 (2005).
 - [20] O. Astafiev et al., Science **327**, 840 (2010).
 - [21] P. Yeh, *Optical Waves in Layered Media*, Wiley-Interscience, New York (1988).
 - [22] N. B. Phillips, A. V. Gorshkov and I. Novikova, Phys. Rev. A **78**, 023801 (2008).
 - [23] P. Lambropoulos and D. Petrosyan, *Fundamentals of Quantum Optics and Quantum Information*, Springer-Verlag, Berlin (2006).
 - [24] The relaxation parameters are found using the transition matrix element relation $\mu_{es} = 0.23\mu_{eg}$ from Ref. [17].

APPENDIX

Inter-atomic scattering interference occurs in a one-dimensional array of superconducting artificial atoms, which leads to oscillations in the electromagnetically induced transparency window width w as a function of the number of atoms n . Here we derive an expression for $w(n)$ that shows the $w \propto \frac{1}{\sqrt{n}}$ behavior with an additional oscillatory modulation term. At the vicinity of zero signal field detuning, i.e. $\delta \approx 0$, the transmission $T(\delta) = T(0)\exp(-\frac{\delta^2}{w^2})$ with $T(0) \approx 1$. Hence, the window width is

$$w^2 = \frac{2}{-\left.\frac{d^2 \ln T}{d\delta^2}\right|_{\delta=0}},$$

where the transmission $T = \left| \frac{1}{M_{11}} \right|^2$. For r the reflection coefficient for a single atom and ϕ the phase shift due to free propagation between a pair of adjacent atoms,

$$\begin{aligned}
M_{11} &= \sum_{j=1,2} G_j F_j^n, \\
G_1 &= \frac{A_+ + B}{2e^{-i\phi} B}, \\
G_2 &= -\frac{A_+ - B}{2e^{-i\phi} B}, \\
F_1 &= \frac{A_- + B}{2e^{i\phi}(r-1)}, \\
F_2 &= \frac{A_- - B}{2e^{i\phi}(r-1)}, \\
A_{\pm} &= \pm e^{2i\varphi}(1-2r) - 1, \\
B &= \sqrt{(e^{2i\varphi} - 1)(e^{2i\varphi}(1-2r)^2 - 1)}.
\end{aligned}$$

Note that the square root in the expression for B may take a plus or minus sign. Changing the sign leads to a swap of expression for G_1 and G_2 as well as for F_1 and F_2 ; thus, the expression for M_{11} is the same for either case. In the following, we obtain an expression for $-\frac{d^2 \ln T}{d\delta^2}$.

$$\begin{aligned}
-\ln T &= \ln \sum_{j=1,2} G_j F_j^n + \text{c.c.}, \\
-\frac{d \ln T}{d\delta} &= \frac{1}{\sum_{j=1,2} G_j F_j^n} \sum_{j=1,2} \left(n G_j \frac{d \ln F_j}{d\delta} + \frac{d G_j}{d\delta} \right) F_j^n + \text{c.c.}, \\
-\frac{d^2 \ln T}{d\delta^2} &= \frac{1}{\sum_{j=1,2} G_j F_j^n} \sum_{j=1,2} \left(G_j \left(\frac{d \ln F_j}{d\delta} \right)^2 n^2 + \left(G_j \frac{d^2 \ln F_j}{d\delta^2} + 2 \frac{d G_j}{d\delta} \frac{d \ln F_j}{d\delta} \right) n + \frac{d^2 G_j}{d\delta^2} \right) F_j^n \\
&\quad - \frac{1}{(\sum_{j=1,2} G_j F_j^n)^2} \left(\sum_{j=1,2} \left(n G_j \frac{d \ln F_j}{d\delta} + \frac{d G_j}{d\delta} \right) F_j^n \right)^2 + \text{c.c.}
\end{aligned}$$

We define

$$\begin{aligned}
a_j &= G_j \left(\frac{d \ln F_j}{d \delta} \right)^2, \\
b_j &= G_j \frac{d^2 \ln F_j}{d \delta^2} + 2 \frac{d G_j}{d \delta} \frac{d \ln F_j}{d \delta}, \\
c_j &= \frac{d^2 G_j}{d \delta^2}, \\
b'_j &= G_j \frac{d \ln F_j}{d \delta}, \\
c'_j &= \frac{d G_j}{d \delta}.
\end{aligned}$$

such that

$$\begin{aligned}
-\frac{d^2 \ln T}{d \delta^2} &= \frac{(a_1 n^2 + b_1 n + c_1) F_1^n + (a_2 n^2 + b_2 n + c_2) F_2^n}{G_1 F_1^n + G_2 F_2^n} - \left(\frac{(b'_1 n + c'_1) F_1^n + (b'_2 n + c'_2) F_2^n}{G_1 F_1^n + G_2 F_2^n} \right)^2 + \text{c.c.} \\
&= \frac{1}{(G_1 F_1^n + G_2 F_2^n)^2} \left(((G_1 F_1^n + G_2 F_2^n)(a_1 F_1^n + a_2 F_2^n) - (b'_1 F_1^n + b'_2 F_2^n)^2) n^2 \right. \\
&\quad + ((G_1 F_1^n + G_2 F_2^n)(b_1 F_1^n + b_2 F_2^n) - 2(b'_1 F_1^n + b'_2 F_2^n)(c'_1 F_1^n + c'_2 F_2^n)) n \\
&\quad \left. + (G_1 F_1^n + G_2 F_2^n)(c_1 F_1^n + c_2 F_2^n) - (c'_1 F_1^n + c'_2 F_2^n)^2 \right) + \text{c.c.} \\
&= 2 \text{Re} \left(\frac{1}{(G_1 F_1^n + G_2 F_2^n)^2} \left((a_2 G_1 + a_1 G_2 - 2b'_1 b'_2) n^2 \right. \right. \\
&\quad + ((b_1 G_1 - 2b'_1 c'_1) F_1^{2n} + (b_2 G_1 + b_1 G_2 - 2b'_1 c'_2 - 2b'_2 c'_1) + (b_2 G_2 - 2b'_2 c'_2) F_2^{2n}) n \\
&\quad \left. \left. + (c_1 G_1 - c_1'^2) F_1^{2n} + (c_2 G_1 + c_1 G_2 - 2c'_1 c'_2) + (c_2 G_2 - c_2'^2) F_2^{2n} \right) \right)
\end{aligned}$$

as $F_1 F_2 = 1$, $a_1 G_1 = b_1'^2$ and $a_2 G_2 = b_2'^2$.

For the chosen parameters (see paper), at $\delta = 0$, we have $F_1 = 0.689 + i0.725$, $F_2 = 0.689 - i0.725$, $G_1 = 3.33 \times 10^{-9} + i3.50 \times 10^{-9}$, $G_2 = 0.689 + i0.725$ and $F_1 - G_2 = -6.94 \times 10^{-5} - i7.30 \times 10^{-5}$; thus, $|G_1| |F_1|^n \ll |G_2| |F_2|^n$ for all n . Also, $a_2 G_1 + a_1 G_2 - 2b'_1 b'_2 = 1.46 \times 10^{-27} - i2.88 \times 10^{-26}$, $b_1 G_1 - 2b'_1 c'_1 = 3.32 \times 10^{-35} - i1.49 \times 10^{-35}$, $b_2 G_1 + b_1 G_2 - 2b'_1 c'_2 - 2b'_2 c'_1 = -2.87 \times 10^{-23} + i5.66 \times 10^{-22}$, $b_2 G_2 - 2b'_2 c'_2 = -1.42 \times 10^{-18} + i6.38 \times 10^{-19}$, $c_1 G_1 - c_1'^2 = -3.40 \times 10^{-28} + i6.71 \times 10^{-27}$, $c_2 G_1 + c_1 G_2 - 2c'_1 c'_2 = 7.01 \times 10^{-20} - i1.39 \times 10^{-18}$ and $c_2 G_2 - c_2'^2 = -7.01 \times 10^{-20} + i1.39 \times 10^{-18}$. Therefore, the n^2 term and the F_1^{2n} terms are insignificant. The simplified expression for the window width in Hz is

$$w \approx \frac{1}{\sqrt{7.10 \times 10^{-19} n + 1.39 \times 10^{-18} (1 - (0.9999)^{2n} \cos 1.62n)}}.$$